

Effects of Pre-reducing Sb-Doped SnO₂ Electrodes in Viologen-Anchored TiO₂ Nanostructure-Based Electrochromic Devices

Seong Mok Cho, Chil Seong Ah, Tae-Youb Kim, Juhee Song, Hojun Ryu, Sang Hoon Cheon, Joo Yeon Kim, Yong Hae Kim, and Chi-Sun Hwang

In this paper, we investigate the effects of pre-reducing Sb-doped SnO₂ (ATO) electrodes in viologen-anchored TiO₂ (VTO) nanostructure-based electrochromic devices. We find that by pre-reducing an ATO electrode, the operating voltage of a VTO nanostructure-based electrochromic device can be lowered; consequently, such a device can be operated more stably with less hysteresis. Further, we find that a pre-reduction of the ATO electrode does not affect the coloration efficiency of such a device. The aforementioned effects of a pre-reduction are attributed to the fact that a pre-reduced ATO electrode is more compatible with a VTO nanostructure-based electrochromic device than a non-pre-reduced ATO electrode, because of the initial oxidized state of the other electrode of the device, that is, a VTO nanostructure-based electrode. The oxidation state of a pre-reduced ATO electrode plays a very important role in the operation of a VTO nanostructure-based electrochromic device because it strongly influences charge movement during electrochromic switching.

Keywords: Electrochromism, nanostructure, viologen, TiO₂, Sb-doped SnO₂.

Manuscript received Apr. 7, 2015; revised Nov. 9, 2015; accepted Feb. 18, 2016.

Seong Mok Cho (corresponding author, smcho@etri.re.kr), Chil Seong Ah (acs@etri.re.kr), Tae-Youb Kim (youb@etri.re.kr), Juhee Song (juhee0309@etri.re.kr), Hojun Ryu (hjryu@etri.re.kr), Sang Hoon Cheon (sh.cheon@etri.re.kr), Joo Yeon Kim (jooyeon.kim@etri.re.kr), Yong Hae Kim (yhakim@etri.re.kr), and Chi-Sun Hwang (hwang-cs@etri.re.kr) are with the ICT Materials & Components Research Laboratory, ETRI, Daejeon, Rep. of Korea.

I. Introduction

Technologies related to both transparency control and reflectance control, which operate in the visible range of the spectrum, are receiving increasing amounts of interest by researchers in related fields because they can be applied to smart windows and other related applications [1]–[10]. Over the past several decades, electrochromism has attracted increasing interest [1]–[6]. Electrochromic materials can be applied to “smart windows” [11]–[13], automobile mirrors, and displays [14]–[16]. However, the slow switching speeds of conventional electrochromic devices have limited their applicability to low-speed domains for decades; slow switching speeds are a result of low Li⁺ ion diffusion rates in thin-films pertaining to electrochromic materials [17].

Recently, ultrafast electrochromic devices utilizing viologen-anchored TiO₂ (VTO) nanostructure-based electrodes have been demonstrated [17], [18]. In such devices, viologen molecules are fixed to the surfaces of TiO₂ nanostructure-based electrodes. Therefore, Li⁺ ion diffusion lengths for electrochromic switching are minimized and sub-second switching speeds can be realized. Since this breakthrough, ultrafast electrochromic devices based on VTO nanostructure-based electrodes have attracted significant attention [19]–[21]; viologen-graphene systems have also drawn much attention [22], [23]. We note here that a counter electrode is a very important component of an electrochromic device. A Sb-doped SnO₂ (ATO) nanostructure is the most promising material for a counter electrode because it can act as a good ion storage layer

[24]. Upon reduction or oxidation of an ATO electrode, any resulting change in color is notably and insignificantly small.

ATO nanoparticles, which form the basis of an ATO electrode's nanostructure, can be synthesized by hydrothermal methods [24]. To fabricate an ultrafast electrochromic device, one must first separately form a VTO nanostructure-based electrode and an ATO electrode prior to any attempts to then combine the two. When it comes to forming the electrodes, a high-temperature treatment within an oxidizing environment is required; therefore, the electrodes will be in an oxidized state upon fabrication due to this environment.

During an electrochromic operation (that is, the operation of an ultrafast electrochromic device), of the two electrodes that make up the device, it is the VTO nanostructure-based electrode that is typically to be reduced while simultaneously oxidizing the ATO electrode; the further oxidation of an ATO electrode is not easy and indeed a high voltage needs to be applied to the device in order to achieve this. Since further oxidation is impractical, we investigate the possibility of pre-reducing an ATO electrode prior to its involvement in the construction phase of an ultrafast electrochromic device. By pre-reducing an ATO electrode, we can lower its level of oxidation prior to it ever being operated within an ultrafast electrochromic device. Thus, during an electrochromic operation, when the time comes to oxidize the ATO electrode, a low voltage needs only to be applied to achieve the desired effect.

With this understanding, we seek to investigate the effects of pre-reducing ATO electrodes in ultrafast electrochromic devices.

Pre-reduction of ATO electrodes is conducted with a potentiostat prior to cell construction. The effects of pre-reduction of ATO electrodes on the electrochromic properties of VTO nanostructure-based electrochromic devices is systematically analyzed.

II. Experiment

A TiO_2 nanoparticle slurry with an average particle size of less than 20 nm was supplied by ENB Korea Co., Ltd., and fluorine-doped SnO_2 (FTO) coated glasses (TEC-15, sheet resistance of $15 \Omega/\square$), supplied by Pilkington Co., Ltd., were used as substrates. Thin films were prepared using the bar-coating method followed by calcination at 450°C for 30 min in air to burn off polymer materials and to form TiO_2 nanostructure-based electrodes. The thicknesses of the nanostructured films were measured using a surface profiler (Alpha-step 500, KLA-Tencor Co.) and the average thickness was $4 \mu\text{m}$.

Methyl viologen, which is deep blue when in a reduced state but transparent when in an oxidized state, was used as the

electrochromic material. Phosphate anchors were formed on the viologen molecules using a process suggested by previous researchers [17]. The phosphate-anchored viologen molecules were fixed to the surfaces of TiO_2 nanostructure-based electrodes using a solution method. The phosphate-anchored viologen molecules were dissolved in a 0.5 mM concentration of ethanol, and TiO_2 nanostructure-based electrodes were dipped in the solution for 20 h, then rinsed in ethanol and dried. The now prepared VTO nanostructure-based electrodes were highly transparent, displaying no color upon visual inspection, meaning the absorbed viologen molecules were still in their natural oxidized state.

Figure 1 shows the cyclic voltammetry results for TiO_2 nanostructure-based electrodes, as measured with a potentiostat (CHI1030, CH Instrument Inc., USA) before and after viologen anchoring. The sweep rate was $5 \text{ mV}\cdot\text{s}^{-1}$. The reference electrode (of the potentiostat) was a Ag/AgCl electrode, and 0.5 M LiClO_4 in propylene carbonate was used as the electrolyte in the measurement. As can be seen in Fig. 1, the current was drastically increased by anchoring viologen to the surfaces of the TiO_2 nanostructure-based electrodes. This occurred because the absorbed viologen molecules took part in oxidation/reduction processes during the cyclic voltammetry measurements. From Fig. 1, it is estimated that the reduction/oxidation potential of viologen is approximately -0.5 V with respect to the Ag/AgCl reference electrode.

ATO nanoparticles were synthesized using a hydrothermal process that has been described in previous reports [24]. The Sb content of the ATO nanoparticles was 5.0 at %. The

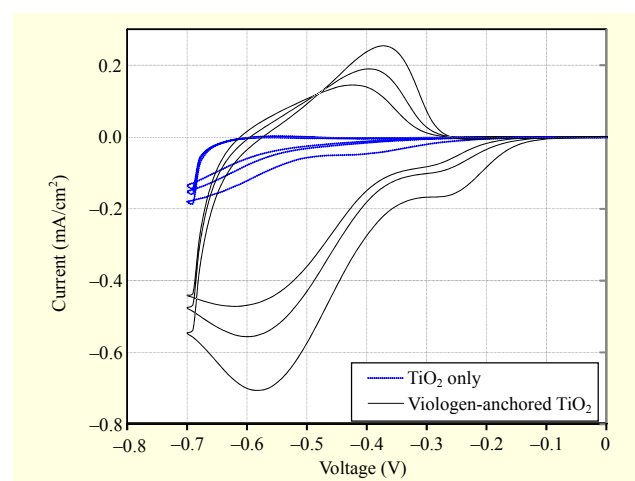


Fig. 1. Cyclic voltammetry results of TiO_2 nanostructure-based electrodes before and after viologen anchoring. Range of voltage sweep for cyclic voltammetry is -0.7 V to 0.5 V with respect to Ag/AgCl reference electrode. Sweep speed is $5 \text{ mV}\cdot\text{s}^{-1}$, and 0.5 M LiClO_4 in propylene carbonate is used as electrolyte. First three cycles for each sample are shown.

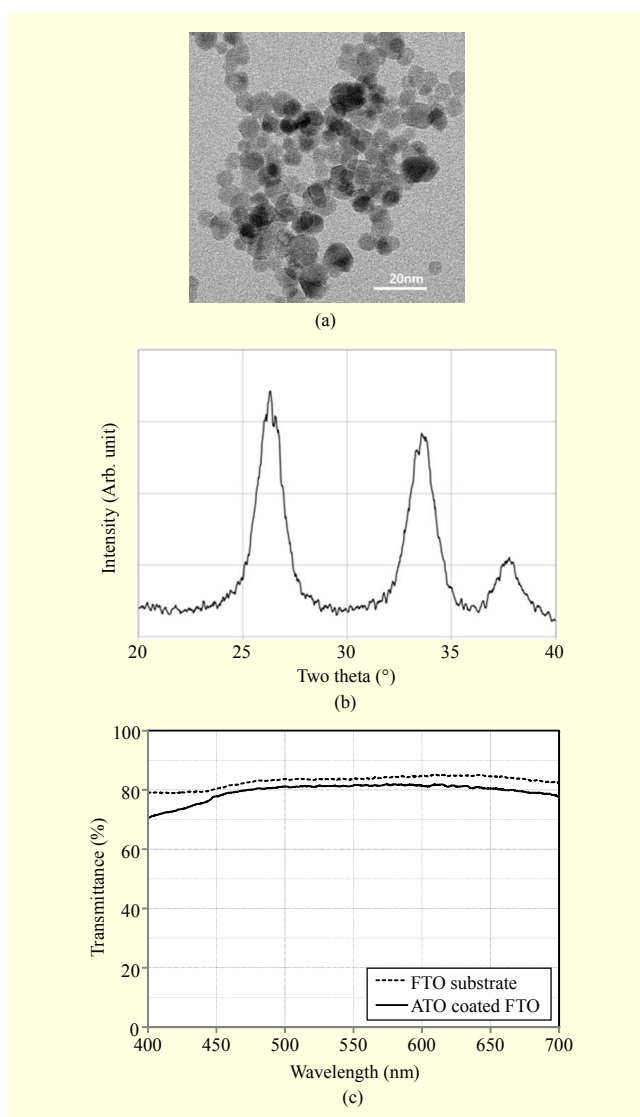


Fig. 2. (a) TEM image of synthesized ATO nanoparticles, (b) X-ray diffraction pattern of synthesized ATO nanoparticles, and (c) transmittance spectrum of ATO electrode.

synthesized nanoparticles were mixed with terpineol, lauric acid, and ethyl cellulose to make a slurry to be used for the bar-coating process. The prepared slurry was bar-coated, as thin films, onto the FTO substrates and dried in air. The dried films were calcined at 450 °C, for 30 min in air to burn off the polymers and make several ATO electrodes. The final thickness of the ATO films was approximately 4 μm. Figure 2 shows a TEM image of the synthesized ATO nanoparticles, an X-ray diffraction (XRD) pattern of the nanoparticles, and the measured transmittances of the prepared ATO films. Note that the average size of an ATO nanoparticle must be very small if it is to be used in the fabrication of a transparent electrode.

A major loss of transmittance occurred because of scattering by the ATO nanoparticles or agglomerates of ATO

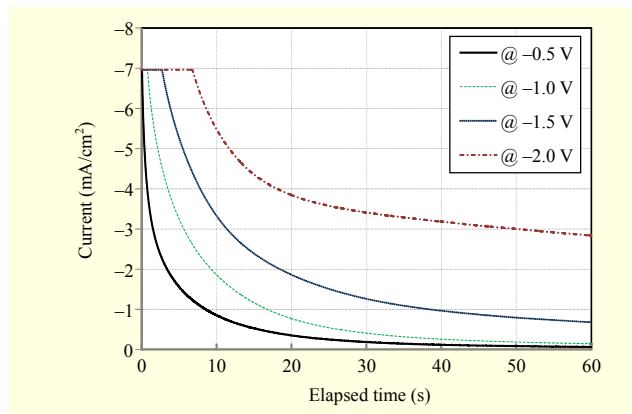


Fig. 3. Amperometric *i-t* results measured during pre-reduction processes.

nanoparticles. Therefore, the smaller the primary ATO nanoparticles, the more transparent a thin film is [25]. The average particle size of the synthesized ATO nanoparticles was less than 10 nm, and the ATO films were very transparent because of the sizes of the primary ATO nanoparticles. The synthesized ATO nanoparticles were crystallites, as can be seen from Fig. 2(b). From the XRD pattern, the crystal structure of the ATO nanoparticles was confirmed to be tetragonal, cassiterite phase SnO₂.

The ATO electrodes were pre-reduced through an amperometric *i-t* method using a potentiostat (CHI1030, CH Instrument Inc., USA) before cell construction. For the pre-reduction, the Ag/AgCl electrode was used as a reference electrode, 0.5 M LiClO₄ in propylene carbonate was used as an electrolyte, and the voltage range of pre-reduction was -0.25 V to -2.0 V, with respect to the Ag/AgCl reference electrode. Figure 3 shows the time-current (*i-t*) graphs measured during the pre-reduction processes for several pre-reduction voltages. As can be seen from the figure, the charging currents related with the pre-reductions decayed almost within 60 s. In the case of pre-reduction voltages higher than -1.5 V, considerable currents were maintained beyond the 60 s mark, but for the most part were considered to be a kind of leakage current. Considering the *i-t* results, the pre-reduction time was fixed to 60 s for all the pre-reduction voltages. The pre-reduced ATO electrodes were rinsed with ethanol and dried. Cell cavities were formed by joining the dried ATO electrodes with the VTO nanostructure-based electrodes using patterned melting films with a thicknesses of 100 μm (Surlyn, Dupont co.). The electrolyte, a 0.5 M LiClO₄ in propylene carbonate, was injected into the cell cavities by vacuum injection, forming the final electrochromic cells. Figure 4(a) presents a schematic showing the vertical structure of the electrochromic devices, and Fig. 4(b) shows photographs of a fabricated device, first in a bleached state and then in a colored state.

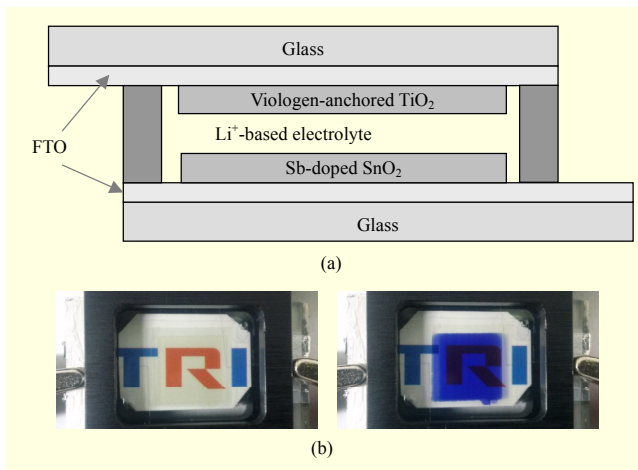


Fig. 4. Schematic showing structure of device, which consists of (a) VTO nanostructure-based electrode and ATO nanostructure-based electrode and (b) photographs of fabricated device in its bleached and colored states.

The devices were $2.0\text{ cm} \times 2.0\text{ cm}$ in size, $1.0\text{ cm} \times 1.0\text{ cm}$ of which was the active area. The electrochromic characteristics of the fabricated devices were measured using an optical measurement system consisting of a light source (DH-2000-BAL, Ocean Optics Inc., USA), optical fibers, and a spectrometer (USB2000+UV-VIS, Ocean Optics Inc., USA). Driving bias was applied by a function generator (Hewlett Packard co., 33120A), dc power supply (Protek co., OPE-303Q), and an isolation board with an operational amplifier. Switching currents during electrochromic operation were recorded using a digital multimeter (Agilent co., 34461A).

III. Results and Discussion

1. Pre-reduction of ATO Electrodes

Figure 5 shows the total amount of charge that flowed into the samples during the pre-reduction processes. The total charge for a sample was obtained by integrating the current over time. Typical switching charge values for the fabricated devices, as measured with a digital multimeter, were less than 0.01 C/cm^2 . Figure 5 shows that the amounts of charge that flowed during the pre-reduction processes were much larger than those associated with device switching.

Pre-reduction involves injecting a positive charge, such as with Li^+ ions, into the ATO electrodes or extracting a negative charge from them. Intuitively, it makes sense that Li^+ ions would be injected into the ATO electrodes since there is no suitable anion to be extracted from the ATO electrodes into the electrolyte. However, not all current flows can be interpreted as charge injected. Some fractions of the currents could be electronic leakage currents. Furthermore, not all of the injected

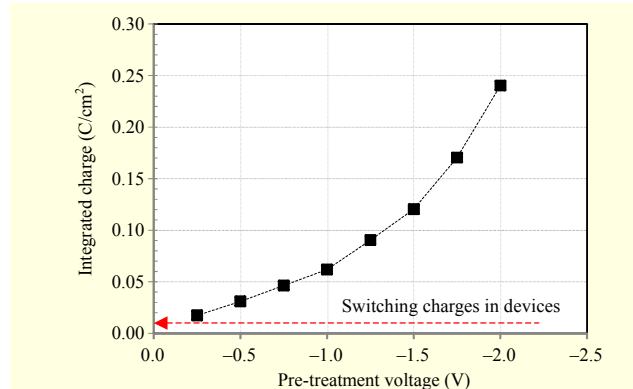


Fig. 5. Amounts of charge that flowed during pre-reduction of ATO electrodes; charge flow was calculated by integrating current data over time obtained from potentiostat.

charges could be maintained until the point of completion of the device fabrication. Some fractions of the injected charges (Li^+ ions) must be oxidized during the latter processes, such as cleaning, cell bonding, and so on. To minimize the re-oxidation of the ATO electrodes, the pre-reduced ATO electrodes were immediately rinsed with ethanol and used to fabricate electrochromic devices.

2. Effects of Pre-reduction on Transmittance Switching

Figure 6 shows the measured transmittance spectra of two of the fabricated devices (of which there were many; however, we do not show all of the results for all the fabricated devices due to space limitations). Figure 6(a) shows the results obtained using operating voltages of -2.5 V (voltage of the VTO nanostructure-based electrode with respect to the ATO electrode) for coloring and $+0.5\text{ V}$ for bleaching. Figure 6(b) shows the spectra obtained using operating voltages of -3.0 V for coloring and $+0.5\text{ V}$ for bleaching. As can be clearly seen from the figure, the coloring level was much deeper in the case of the device with the pre-reduced ATO electrode, and the difference between the two devices featured was larger when a coloring voltage of -2.5 V was used. It is assumed that the reason for these differences is that a pre-reduced ATO electrode can more easily release a charge (become oxidized) than a non-pre-reduced ATO electrode. Therefore, the device made with a pre-reduced ATO electrode can be operated by a lower driving voltage and become more deeply colored. Using an operating voltage of -3.0 V , the device made with the non-pre-reduced ATO electrode also becomes deeply colored. This means that the operating voltage was high enough to extract charges even in the non-pre-reduced case.

Figure 7 shows the amperometric $i-t$ results measured with the potentiostat for both the non-pre-reduced ATO electrode and the pre-reduced ATO electrode. The measurements were

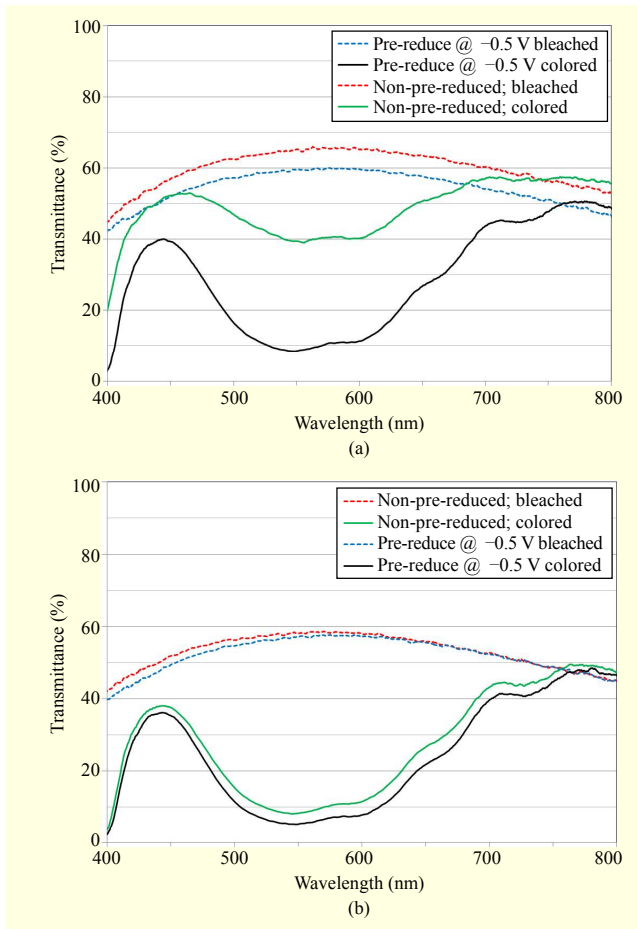


Fig. 6. Transmittance spectra of devices: (a) colored at -2.5 V and bleached at $+0.5$ V and (b) colored at -3.0 V and bleached at $+0.5$ V.

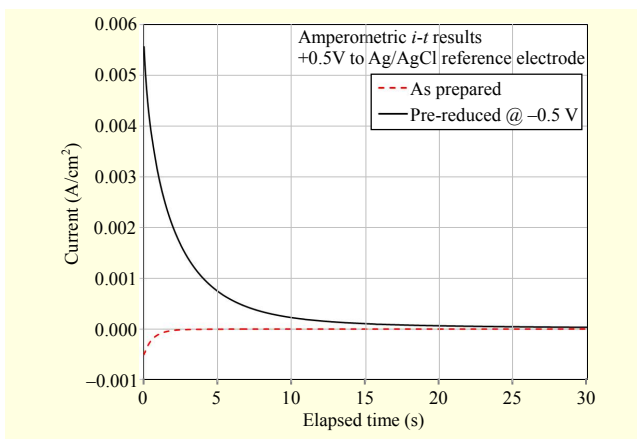


Fig. 7. Amperometric $i-t$ results for non-pre-reduced ATO electrode and pre-reduced ATO electrode. Currents were monitored at constant voltage of $+0.5$ V, with respect to Ag/AgCl reference electrode, using potentiostat. 0.5 M LiClO_4 in propylene carbonate was used as electrolyte.

performed by monitoring the current at a constant voltage of $+0.5$ V (with respect to the Ag/AgCl reference electrode). For

the measurements, 0.5 M LiClO_4 in propylene carbonate was used as the electrolyte. As can be seen from the figure, the pre-reduced ATO electrode released charge and was oxidized under the aforementioned voltage conditions. The non-pre-reduced ATO electrode, however, was not oxidized; rather, it was slightly reduced under the same conditions. These results mean that the non-pre-reduced ATO electrode was strongly oxidized and that it has a strong tendency to be reduced. Therefore, a higher voltage is required to further oxidize the non-pre-reduced ATO electrode; thus, any electrochromic devices made with such an ATO electrode will have a much higher operating voltage than any that are made with the pre-reduced ATO electrode.

3. Hysteresis of Coloration

Figure 8 shows transmittance data obtained from the fabricated devices at a wavelength of 550 nm and their

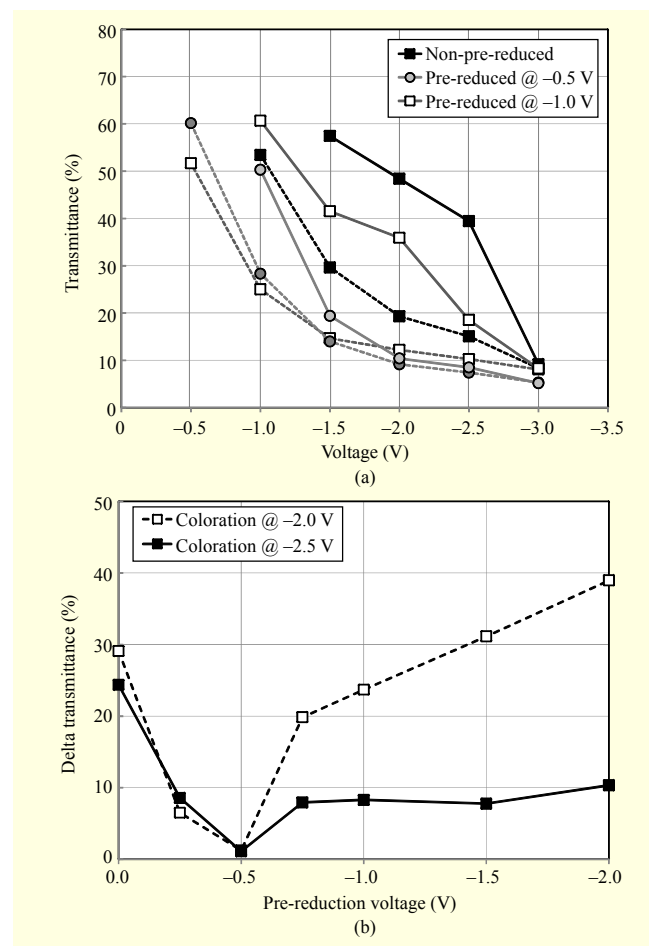


Fig. 8. (a) Transmittances of fabricated devices in colored states at wavelength of 550 nm and (b) differences in transmittance between colored states measured with increasing voltage and decreasing voltage.

hysteresis profiles. The results from three kinds of fabricated device made with different pre-reduction conditions, not pre-reduced, reduced @ -0.5 V, and reduced @ -1.0 V, respectively, are displayed in the figure. The measurements were performed with a fixed bleaching voltage of $+0.5$ V and a variable coloring voltage. Transmittances were measured after switching at a frequency of 0.2 Hz for 5 min to stabilize at each coloring voltage. Measurements were taken while increasing the coloring voltage from -0.5 V to -3.0 V in 0.5 V steps, then decreasing it back to -0.5 V using the same steps. The solid lines in the figure show the results obtained when increasing the operation voltage; the dotted lines show those obtained when decreasing the voltage. It can be seen from the figure that the results obtained when increasing the operating voltage are quite different from those obtained when decreasing the operating voltage. In the case of the device fabricated with the non-pre-reduced ATO electrode, when increasing the coloring voltage, the device was not deeply colored, until -3.0 V. However, after a coloring voltage of -3.0 V was used, the device was deeply colored at lower voltages; its transmittance was less than 20% when a coloring voltage of -2.0 V was used. Large differences were observed between the increasing voltage curve (solid line) and the decreasing voltage curve (dotted line) of this device. Conversely, the device fabricated with the pre-reduced ATO electrode @ -0.5 V was deeply colored at lower coloring voltages and the differences between the increasing voltage curve (solid line) and the decreasing voltage curve (dotted line) were much smaller than those of the device fabricated with the non-pre-reduced ATO electrode.

The device with the pre-reduced ATO electrode @ -1.0 V showed weaker colorations than the device with the pre-reduced ATO electrode @ -0.5 V when increasing the voltage. However, when decreasing the voltage, it showed deep colorations similar with the pre-reduced ATO electrode @ -0.5 V. One interesting property these devices demonstrated is that if the transmittance was measured again immediately after the first measurement then the devices were not colored along the increasing voltage curve (solid line) but were colored along the decreasing voltage curve (dotted line). The devices, after being colored at -3.0 V, showed very different voltage characteristics. Figure 8(b) shows the differences in transmittance results between the increasing voltage curve (solid line) and the decreasing voltage curve (dotted line) as a function of the pre-reduction voltage. As can clearly be seen from the figure, the pre-reduced ATO electrode @ -0.5 V showed the minimum hysteresis characteristics.

4. Effects of Storage Time

Figure 9 shows the effects of storage time for the device

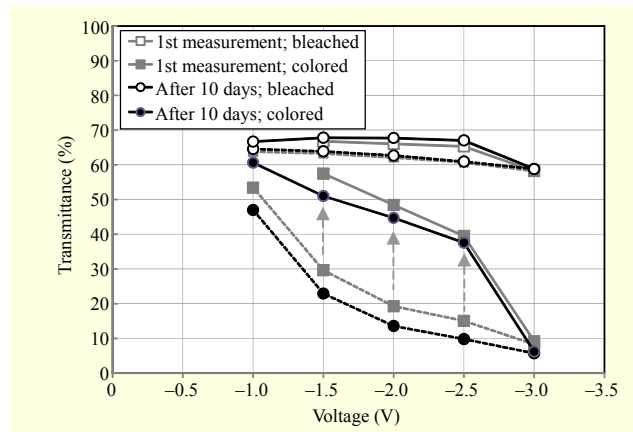


Fig. 9. Transmittances at 550 nm of device made with non-pre-reduced ATO electrode, demonstrating aging effects of devices.

made with the non-pre-reduced ATO electrode. The measurement was taken using the same method that was used to obtain the data in Fig. 8. After taking the measurements shown in Fig. 8, the devices were kept for 10 days in a glove box and then re-examined using the same methods. The stored devices showed very similar characteristics to those of the fresh (prior to being operated) devices despite being previously operated at high coloration voltages (-3.0 V). This can be understood as a result of the charge carriers, which were mobilized by the high voltages used in the previous operation, becoming gradually immobilized with time. Coloring of the fresh devices requires the extraction of a positive charge from the ATO electrode, which is initially in an oxidized state. The ATO electrode requires further oxidation, which is not easy to achieve. However, applying a high voltage (-3.0 V) to an electrochromic device can extract and mobilize charge carriers from its ATO electrode and result in the further oxidation of the electrode. Charge carriers become mobile and induce device coloration at lower coloring voltages for a time. Nevertheless, the now over-oxidized ATO electrode is not stable and tends to revert to its original state. Therefore, mobilized charge carriers are gradually immobilized and the ATO electrode is restored to its original state over time.

Figure 10 shows the results of the same experiment performed on the device made with the pre-reduced ATO electrode. As can be seen from the figure, the device with the pre-reduced ATO electrode can be colored at lower voltages, and the effects of the storage time are very small compared to those of the device fabricated with the non-pre-reduced ATO electrode. This means that the charge carriers of the pre-reduced ATO electrode are mobile at lower voltages and much more stable. The pre-reduced ATO electrode, which is initially in a reduced state, can easily release the charges and become oxidized. The oxidized state is stable and the charges cannot be

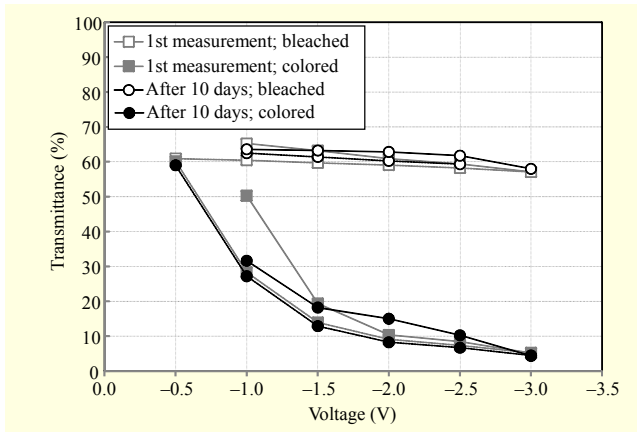


Fig. 10. Transmittances at 550 nm of device made with pre-reduced ATO electrode, demonstrating aging effects of devices.

immobilized.

5. Speed of Transition

Figures 11(a) and 11(b) show transmittance data obtained at a wavelength of 550 nm as a function of time when the featured devices were operated under biases of -2.5 V for coloring and $+0.5$ V for bleaching, and a switching frequency of 1 Hz was used. Figure 10(c) shows the time needed for a 90% change in the level of transmittance (transition time) to occur. Most of the devices, except for the device with the pre-reduced ATO electrode at -2.0 V, show very high transmittance switching speeds; coloring and bleaching occur in less than 100 ms. As can be seen from Figs. 10(a) and 10(b), increasing the pre-reduction voltage resulted in minute increases in tailing during the coloring operation. Severe pre-reduction at high voltages, such as -2.0 V, results in a substantial slowing of the bleaching operation. The speeds of the coloring and bleaching of the devices did not change significantly when the pre-reduction voltage was less than -1.5 V. In Fig. 10(c), it can be seen that bleaching transition time slightly increased when pre-reduction voltages of -0.5 V to -1.5 V were used. This is not because of an actual slowing of the devices but because of an increase in the amplitude of transmittance change that resulted from the pre-reduction. In fact, the slopes of the changes observed in optical densities over time during electrochromic switching were the same for each device. The slowing of devices with pre-reduced ATO electrodes at voltages higher than -1.5 V is expected to be related to damage to the ATO electrodes. Damage to the ATO electrodes might have resulted from either the severe voltage used for pre-reduction or re-oxidation of the injected Li^+ ions following the pre-reduction process. Because excessive pre-reductions induce tailings in the coloring operation and slow

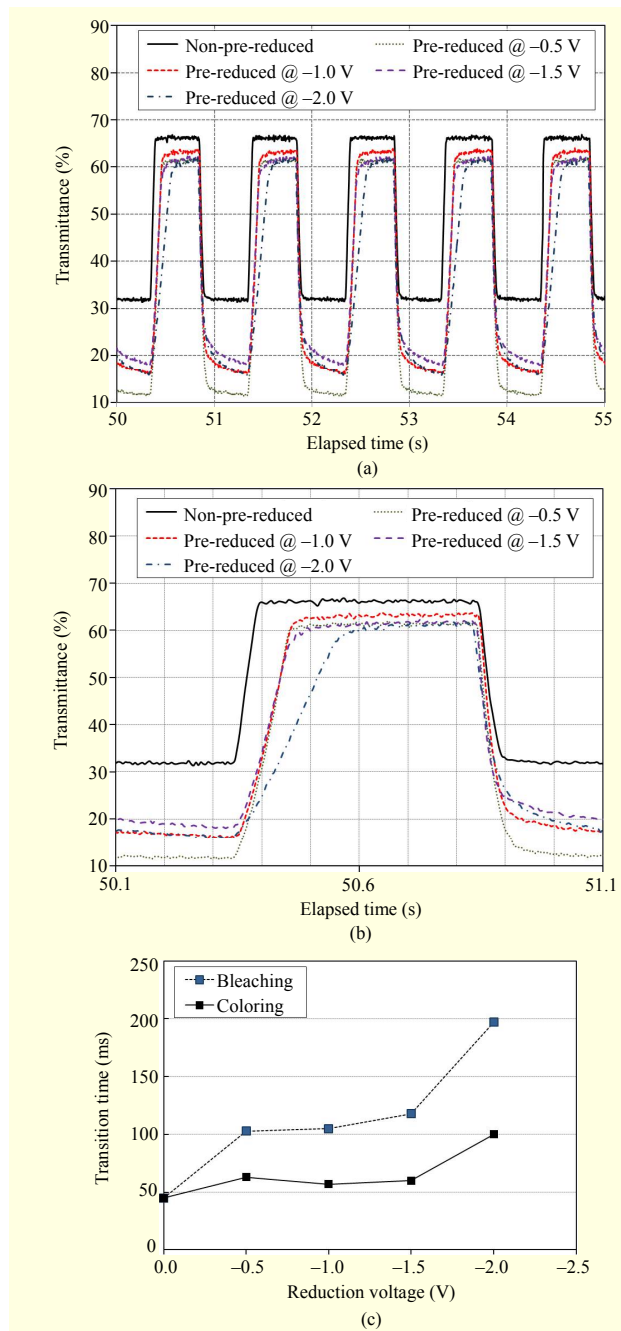


Fig. 11. Plots of (a) transmittance changes of devices at wavelength of 550 nm, (b) magnified graph of (a), which shows single cycle of switching, (c) required times for 90% bleaching and coloring transitions. Bias used for coloration was -2.5 V and that for bleaching was $+0.5$ V; operating frequency was 1 Hz.

the speeds of the devices, the best pre-reduction voltage for the present experimental environments is -0.5 V.

6. Coloration Efficiency

Figure 12 shows how the optical densities of the devices

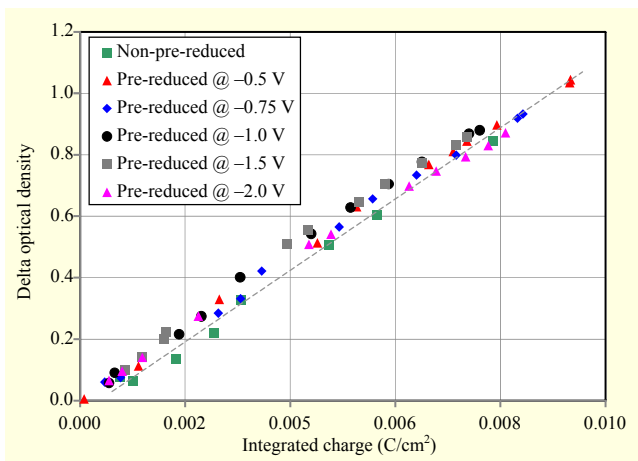


Fig. 12. Plot of optical density changes observed in devices at wavelength of 550 nm vs. total switching charge. Various devices fabricated with pre-reduced ATO electrodes under various conditions. Results of various coloring voltages, in range of -1.0 V to -3.0 V, have been plotted in this figure.

change with the total switching charge when operated under various coloring voltages. Total charges were obtained by integrating over time the switching currents recorded using a digital multimeter, which was connected in series to an electrochromic device. The change in optical density was calculated as follows:

$$\Delta OD = \log \frac{T_{\text{Bleached}}}{T_{\text{colored}}}, \quad (1)$$

where ΔOD is the change in optical density during electrochromic switching, T_{Bleached} is the transmittance (@ 550 nm) of the bleached state, and T_{colored} is that of the colored state. The change in reflectance that occurred during electrochromic switching was minimal, and thus it was neglected in the calculation of the change in optical density. As can be seen from the figure, all data points fell on a single straight line. The slope of the line corresponds to the coloration efficiency of the devices. From the figure, it is clear that coloration efficiencies are almost the same, regardless of the pre-reduction conditions used for the ATO electrodes and operating voltages. The typical coloration efficiency value of our devices was approximately $120 \text{ cm}^2/\text{C}$. That was not affected by the pre-reduction of the ATO electrodes. In some respects, this is not unexpected, because ATO is not an electrochromic species. The pre-reduction of ATO electrodes only influences the movements of the switching charges by changing the oxidation state of the ATO electrodes; it does not influence the coloration efficiency. The coloration efficiency conceptually refers to the change in optical density by a unit switching charge and is basically governed by the electrochromic species. The results in Fig. 12 clearly show that

an electrochromic device is current-operated and that the characteristics of its current operation are not influenced by the state of an ATO electrode.

IV. Conclusion

The effects of the pre-reduction of Sb-doped SnO_2 (ATO) electrodes in viologen-anchored TiO_2 nanostructure-based electrochromic devices were investigated.

The device with the non-pre-reduced ATO electrode needed further oxidation for the coloring operation. However, upon operating the device at a high voltage (for coloring operation), the device showed signs of significant hysteresis. Conversely, the device made with the pre-reduced ATO electrode could be operated at lower voltages more stably and showed less pronounced hysteresis. These results indicate that the oxidation state of the counter electrode plays a very important role in the device operation and that the state of the counter electrode should be accurately controlled. We have shown that the pre-reduction of an ATO electrode bears no significant impact upon the coloration efficiency of the device in which it is employed; rather, it only affects the state of the electrode itself. More specifically, it affects the charge movement during electrochromic switching.

The fabricated devices can be considered potentially applicable as a light shutter for a transparent display or as a smart window, if a scale-up of the devices were to be made. The fabrication process is based on the slurry coating process; therefore, it is relatively easy to meet the requirement of a large scale without the need for huge investment costs.

Acknowledgement

This work was supported by Institute for Information & communications Technology Promotion (IITP) grant funded by the Korea government (MSIP) (B0101-16-0133, the core technology development of light and space adaptable energy-saving I/O platform for future advertising service).

References

- [1] C.G. Granqvist, "Handbook of Inorganic Electrochromic Materials," Amsterdam, Netherlands: Elsevier, 1995.
- [2] C.G. Granqvist, "Progress in Electrochromics: Tungsten Oxide Revisited," *Electrochimica Acta*, vol. 44, no. 18, May 1999, pp. 3005–3015.
- [3] C.G. Granqvist, "Electrochromic Tungsten Oxide Films: Review of Progress 1993–1998," *Solar Energy Mater. Solar Cells*, vol. 60, no. 3, Jan. 2000, pp. 201–262.
- [4] D.R. Rosseinsky and R.J. Mortimer, "Electrochromic Systems

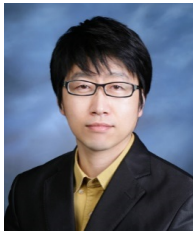
- and the Prospects for Devices,” *Adv. Mater.*, vol. 13, no. 11, June 2001, pp. 783–793.
- [5] N.M. Rowley and R.J. Mortimer, “New Electrochromic Materials,” *Sci. Progress*, vol. 85, no. 3, Aug. 2002, pp. 243–262.
- [6] C.G. Granqvist, “Electrochromic Materials Out of a Niche,” *Nature Mater.*, vol. 5, no. 2, Feb. 2006, pp. 89–90.
- [7] K. Tajima et al., “Flexible All-solid-state Switchable Mirror on Plastic Sheet,” *Appl. Physics Lett.*, vol. 92, 2008, pp. 041912-1–041912-3
- [8] S. Araki et al., “Electrochemical Optical-Modulation Device with Reversible Transformation between Transparent, Mirror, and Black,” *Adv. Mater.*, vol. 24, no. 23, 2012, pp. OP122–OP126.
- [9] T.-Y. Kim et al., “Electrochromic Device for the Reversible Electrodeposition System,” *J. Inf. Display*, vol. 15, no. 1, Jan. 2014, pp. 13–17.
- [10] T.-Y. Kim et al., “Driving Mechanism of High Speed Electrochromic Devices by Using Patterned Array,” *Solar Energy Mater. Solar Cells*, vol. 145, no. 1, Feb. 2016, pp. 76–82.
- [11] G.A. Niklasson and C.G. Granqvist, “Electrochromics for Smart Windows: Thin Films of Tungsten Oxide and Nickel Oxide, and Devices Based on These,” *J. Mater. Chemistry*, vol. 17, no. 2, 2007, pp. 127–156.
- [12] R. Baetens, B.P. Jelle, and A. Gustavsen, “Properties, Requirements and Possibilities of Smart Windows for Dynamic Daylight and Solar Energy Control in Buildings: A State-of-the-art Review,” *Solar Energy Mater. Solar Cells*, vol. 94, no. 2, Feb. 2010, pp. 87–105.
- [13] A. Llodes et al., “Tunable Near-Infrared and Visible-Light Transmittance in Nanocrystal-in-Glass Composites,” *Nature*, vol. 500, Aug. 2013, pp. 323–326.
- [14] P. Bonhôte et al., “Nanocrystalline Electrochromic Displays,” *Displays*, vol. 20, no. 3, Nov. 1999, pp. 137–144.
- [15] T. Yashiro et al., “53: Novel Design for Color Electrochromic Display,” *SID Symp. Dig. Techn. Papers*, vol. 42, no. 1, June 2011, pp. 42–45.
- [16] D. Corr et al., “Coloured Electrochromic Paper-Quality Displays Based on Modified Mesoporous Electrodes,” *Solar State Ionics*, vol. 165, no. 1–4, Dec. 2003, pp. 315–321.
- [17] D. Cummins et al., “Ultrafast Electrochromic Windows Based on Redox-Chromophore Modified Nanostructured Semiconducting and Conducting Films,” *J. Physical Chemistry B*, vol. 104, no. 48, 2000, pp. 11449–11459.
- [18] M. Gratzel, “Material Science: Ultrafast Color Displays,” *Nature*, vol. 409, Feb. 2001, pp. 575–576.
- [19] Y. Rong et al., “New Effective Process to Fabricate Fast Switching and High Contrast Electrochromic Device Based on Viologen and Prussian Blue/Antimony Tin Oxide Nanocomposites with Dark Colored State,” *Electrochimica Acta*, vol. 56, no. 17, July 2011, pp. 6230–6236.
- [20] J. Carcia-Cañadas et al., “Dynamic Behavior of Viologen-Activated Nanostructured TiO₂: Correlation between Kinetics of Charging and Coloration,” *Electrochimica Acta*, vol. 49, no. 5, Feb. 2004, pp. 745–752.
- [21] S.Y. Choi et al., “Electrochromic Performance of Viologen-Modified Periodic Mesoporous Nanocrystalline Anatase Electrodes,” *Nano Lett.*, vol. 4, no. 7, 2004, pp. 1231–1235.
- [22] B. Gadgil et al., “A Facile One Step Electrostatically Driven Electrocodeposition of Polyviologen–Reduced Graphene Oxide Nanocomposite Films for Enhanced Electrochromic Performance,” *Carbon*, vol. 89, Aug. 2015, pp. 53–62.
- [23] E. Hwang et al., “An Electrolyte-Free Flexible Electrochromic Device Using Electrostatically Strong Graphene Quantum Dot–Viologen Nanocomposites,” *Adv. Mater.*, vol. 26, no. 30, June 2014, pp. 5129–5136.
- [24] H.J. Kim et al., “Formation of Ultrafast-Switching Viologen-Anchored TiO₂ Electrochromic Device by Introducing Sb-Doped SnO₂ Nanoparticles,” *Solar Energy Mater. Solar Cells*, vol. 93, no. 12, Dec. 2009, pp. 2108–2112.
- [25] S.Y. Chae et al., “Preparation of Size-Controlled TiO₂ Nanoparticles and Derivation of Optically Transparent Photocatalytic Films,” *Chemistry Mater.*, vol. 15, no. 17, 2003, pp. 3326–3331.



Seong Mok Cho received his BS, MS, and his PhD degrees in materials engineering from Pohang University of Science and Technology, Rep. of Korea, in 1992, 1994, and 2001, respectively. From February 1994 to January 1996, he worked as a research engineer with the Semiconductor Division of Samsung Electronics, Kiheung, Rep. of Korea. He has been with ETRI, as a principal researcher since 2001. His current research interests include electrochromic devices, holographic displays, and sensor devices.



Chil Seong Ah received his BS degree in chemistry from Hanyang University, Seoul, Rep. of Korea, in 1996 and his MS and PhD degrees in chemistry from Seoul National University, Rep. of Korea, in 1998 and 2003, respectively. From March 2003 to August 2005, he worked as a postdoctoral fellow at the Korea Research Institute of Standards and Science, Daejeon, Rep. of Korea. He has been with ETRI a principal researcher, since 2005. His current research interests include sensor, electrochromic and reflective.



Tae-Youb Kim received his MS degree in physics from Yonsei University, Seoul, Rep. of Korea, in 2000 and his PhD in electronic engineering from Tohoku University, Sendai, Japan, in 2011. He has been with ETRI, as a principal researcher, since 2000. His current research interests include electrochromic devices, holographic displays, and sensor devices.

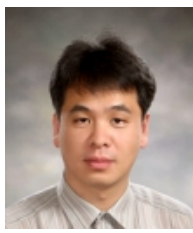


Juhee Song received her BS degree in chemistry from Chungnam National University, Daejeon, Rep. of Korea, in 2011. Since 2011, she has been working at ETRI. Her research interests include electrochromic devices and biosensors.



Hojun Ryu received his BS, MS, and his PhD degrees in material science and engineering from Seoul National University, Rep. of Korea, in 1986, 1993, and 1998, respectively. From August 1999 to February 2001, he worked as a postdoctoral research fellow at the University of Texas at Austin, USA. He has been with ETRI

as a senior research staff member, since 2001. He has conducted research in the fields of MEMS devices and nanostructure fabrication of functional materials. Currently, he is involved in several research projects including the development of a reflective display and future display mode. He is an editorial committee member of the Journal of the Korean Institute of Electrical and Electronic Material Engineers. His current research interests include electrochromic devices, holographic displays, and sensor devices.



Sang Hoon Cheon received his BS, MS, and PhD degrees in electronics engineering and computer science from the Korea Advanced Institute of Science and Technology, Daejeon, Rep. of Korea, in 1993, 1995, and 2001, respectively. In 2001, he joined Knowledge*On, Inc., Rep. of Korea, where he was involved in

the 6-inch InGaP/GaAs HBT foundry service industry. From 2001 to 2003, he worked on large signal modeling for microwave devices, and from 2004 to 2005, he worked on the development of power amplifiers for WCDMA systems. In 2006, he began work at ETRI, where he participated in the development of a micro-bolometer for infrared focal plane arrays. His current research interests include wireless power transfer systems and drive circuits for electrochromic devices.



Joo Yeon Kim received her PhD in material science and engineering from Hannam University, Daejeon, Rep. of Korea, in 2006. She then went on to work at the Korean Institute of Materials and Machinery, Daejeon, Rep. of Korea, as a research fellow, where she focused on improving the hydrophilic/phobic properties of materials used in UV nanoimprinting lithography (UV-NIL). In 2007, she joined Prof. Juergen Brugger's group at Ecole Polytechnique Fédérale de Lausanne, Switzerland, as a postdoctoral research fellow with interests in inkjet printing for micro-/opto-electronic applications with electrical/optical grade polymers and polymer nanocomposites. Since 2010, she has been at ETRI, as a senior researcher, and has been working on reflective displays in connection with nanoparticles, polymers, and graphene.



Yong Hae Kim received his BS, MS, degrees and PhD degrees in physics from the Korea Advanced Institute of Science and Technology, Daejeon, Rep. of Korea, in 1991, 1993, and 1997, respectively. From 1997 to 2001, he worked as a research engineer at Hynix Semiconductor, Icheon, Rep. of Korea, where

he was responsible for the development of DRAM devices made from 0.15 μm technology. Since 2001, he has been with ETRI. His current research interests include spatial light modulators, 3D display systems, and metamaterials.



Chi-Sun Hwang received his BS degree in physics from Seoul National University, Rep. of Korea, in 1991 and his PhD in physics from the Korea Advanced Institute of Science and Technology, Daejeon, Rep. of Korea, in 1996.

From 1996 to 2000, he worked on DRAM devices with 0.18 μm technology at Hyundai Semiconductor Inc., Icheon, Rep. of Korea. Since 2000, he has been with ETRI, Rep. of Korea. His research interests include display technology based on active matrix flat panel displays using TFTs, especially oxide TFTs, environment-adaptive displays, digital holography, and novel switching devices.